Supplementary material for: "A statistical method for revealing form-function relations in biological networks"

Andrew Mugler

Department of Physics, Columbia University, New York, NY 10027

Boris Grinshpun

Department of Applied Physics and Applied Mathematics, Columbia University, New York, NY 10027

Riley Franks

Department of Applied and Computational Mathematics, California Institute of Technology, Pasadena, CA 91125

Chris H. Wiggins

Department of Applied Physics and Applied Mathematics, Center for Computational Biology and Bioinformatics, Columbia University, New York, NY 10027

Contents

This document contains details on the set of networks studied, the regulatory model, the optimization procedure, and the statistical analysis used to identify exemplars among non-redundant groups of topological features. Additionally, it includes further background on information theory and the linear noise approximation. Finally, it presents numerical and analytic results as referenced in the main text, including numerical tests of the robustness of results to uniformity assumptions made in the statistical analysis, statistical validation of an analytically derived functional constraint, and analytic results on the ability of networks to perform XOR functions.

NETWORKS

Many researchers over the past decades have begun to focus on the description of a given biological system not in terms of the isolated functions of its independent components, but in terms of the collective function of the network of interacting components as a whole. A central example of such a network is that describing interactions among genes: many genes produce proteins called transcription factors, whose role is to influence the protein production of other genes. The goal of the present study is, for a set of such networks, to develop a statistical method for determining the extent to which the topology of the network correlates with the function(s) it performs. In this section we describe the set of networks considered, including presentation of its combinatorics.

We consider the set of networks consisting of two transcription factors A and B, each of which can be chemically inhibited, each of which is regulated by itself, the other, or both, and one of which regulates the expression of a fluorescent output gene G (see Fig. 1A of the main text). We distinguish between up- and down-regulating edges, and, in the case of more than one regulatory input edge, between additive and multiplicative interaction of the transcription factors (see model in next section). This gives a set of 160 networks, as described by the combinatorics here.

There are six ways in which the three possible feedback edges illustrated in Fig. 1A of the main text can appear such that species A remains regulated. In 2 configurations (Figs. S1A-B), both A and B are singly regulated, and there are a total of 3 edges per configuration, each of which can be up- or down-regulating. The number of networks is thus [number of configurations]$\times$[2^(number of edges)] = [2] $\times$ [$2^{(3)}$] = 16.

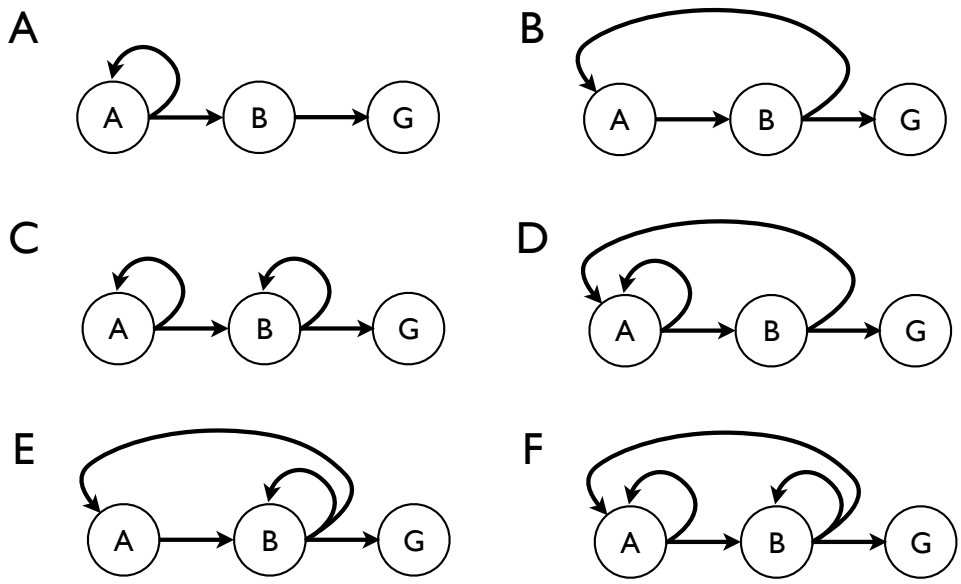

FIG. S1: The six possible topological configurations of the networks studied.

In 3 configurations, (Fig. S1C-E), one of A and B is singly regulated while the other is doubly regulated. In the case of double regulation, the interaction between transcription factors is either (i) additive, in which the signs (up or down) of the two regulatory edges are independent, giving 4 possibilities, or (ii) multiplicative, in which the two regulatory edges have the same sign, giving 2 possibilities (see model in next section), for a total of 6 possibilities. The number of networks is thus [number of configurations]×[2^(number of singly regulated nodes)]×[6^(number of doubly regulated nodes)] = $[3] \times [2^{(2)}] \times [6^{(1)}] = 72$.

In the last configuration (Fig. S1F), both A and B are doubly regulated, and the number of networks is [number of configurations]×[2^(number of singly regulated nodes)]×[6^(number of doubly regulated nodes)] = $[1] \times [2^{(1)}] \times [6^{(2)}] = 72$. This gives a total of $16 + 72 + 72 = 160$ networks.

GENE REGULATION

A regulatory network is most simply described using a dynamical system whose degrees of freedom are the concentrations of its constituent proteins. The nature of the interactions is then determined by the functional form of regulatory production terms on the righthand side of the dynamical system. In this study we formulate production terms under a statistical

mechanical model [1–3] that has been shown to capture diverse functionality in the case of combinatorial regulation [1].

Because many proteins are present in cells in as few as tens or hundreds of copies [4], a deterministic dynamical system, which ignores intrinsic fluctuations around mean protein concentrations, can provide an insufficient description of the biological system when copy numbers are low. Ideally one instead seeks to solve the *master equation*, which describes the dynamics of the *probability* of observing given protein numbers. Unfortunately, almost all master equations describing regulatory networks, including the set of small networks we study here, are intractable analytically. As a result, several techniques to simulate [5] or approximate [6] the master equation have been developed; we here employ the *linear noise approximation* (LNA). Since the LNA does not rely on sampling (in contrast to simulation techniques), it is computationally efficient, which makes feasible the many-parameter optimization performed in this study.

The LNA is a second-order expansion of the master equation, with the first-order terms recovering the deterministic description. Therefore, in the present section, we first describe in detail the regulatory model used in the deterministic system; then we describe the LNA and its application to our networks.

Deterministic description: Dynamical system

As in Eqn. 1 of the main text, the mean protein numbers of the three species are described by the following deterministic dynamics (for notational brevity the bars have been dropped — i.e. the quantities $\bar{A}$, $\bar{B}$, and $\bar{G}$ have been changed to A, B, and G — and the regulation terms φ_A, φ_B, and φ_G have been relabeled α, β, and γ, respectively):

$$\frac{1}{R_A}\frac{dA}{dt} = \alpha(a,b) - A, \tag{1}$$

$$\frac{1}{R_B}\frac{dB}{dt} = \beta(a,b) - B, \tag{2}$$

$$\frac{1}{R_G}\frac{dG}{dt} = \gamma(b) - G, \tag{3}$$

where $a = \{A/x, A\}$ when the first inhibitor is {present, absent}, $b = \{B/y, B\}$ when the second inhibitor is {present, absent}, and the R_j are degradation rates ($j \in \{A, B, G\}$). The parameters $x > 1$ and $y > 1$ incorporate the inhibition by reducing the effective concentra-

tions of the proteins. This gives a total of four chemical input states $c \in \{--, -+, +-, ++\}$, each state describing whether each of the two inhibitors is present $(+)$ or absent $(-)$.

Stability

Steady state solutions of the dynamical system in Eqns. 1-3 are stable fixed points, i.e. points at which the all eigenvalues of the Jacobian have negative real part. The Jacobian of the system is

$$J = \begin{pmatrix} \frac{\partial \alpha}{\partial A} - 1 & \frac{\partial \alpha}{\partial B} & 0 \\ \frac{\partial \beta}{\partial A} & \frac{\partial \beta}{\partial B} - 1 & 0 \\ 0 & \frac{\partial \gamma}{\partial B} & -1 \end{pmatrix}. \tag{4}$$

Its eigenvalues are

$$\lambda_{1,2} = \frac{1}{2}\left[\frac{\partial \alpha}{\partial A} + \frac{\partial \beta}{\partial B} - 2 \pm \sqrt{\left(\frac{\partial \alpha}{\partial A} - \frac{\partial \beta}{\partial B}\right)^2 + 4\frac{\partial \alpha}{\partial B}\frac{\partial \beta}{\partial A}}\right] \tag{5}$$

and $\lambda_3 = -1$. At stable fixed points $\text{Real}\{\lambda_{1,2}\} < 0$; equivalently the determinant of Eqn. 4, which is real and equal to the product of the eigenvalues, must be negative:

$$\Delta \equiv \det(J) = \lambda_1\lambda_2\lambda_3 = \frac{\partial \alpha}{\partial B}\frac{\partial \beta}{\partial A} - \left(\frac{\partial \alpha}{\partial A} - 1\right)\left(\frac{\partial \beta}{\partial B} - 1\right) < 0. \tag{6}$$

We note that because we have nondimensionalized the right-hand side of the dynamical system, the stability analysis presented here is applicable strictly for the simplified case $R_A = R_B = R_G$.

Regulation terms

The regulatory model is that of Buchler et al. [1], in which the protein production is proportional to the probability that the RNA polymerase (RNAp) is bound to the promoter of interest. This probability is formulated thermodynamically, i.e. by enumerating and statistically weighting all ways in which transcription can and cannot occur.

For our networks, the regulation terms α, β, and γ are

$$\alpha(a,b) = \frac{s_A}{R_A} p_A(a,b), \tag{7}$$

$$\beta(a,b) = \frac{s_B}{R_B} p_B(a,b), \tag{8}$$

$$\gamma(b) = \frac{s_G}{R_G} p_G(b), \tag{9}$$

where the s_j are promoter strengths, and the probabilities of transcription p_j are given by

$$p_j = \frac{Z^j_{\text{on}}}{Z^j_{\text{on}} + Z^j_{\text{off}}}. \tag{10}$$

The partition functions Z^j_{on} and Z^j_{off} describe all the ways that transcription can occur and not occur, respectively, at the promoter region of gene j. As presented in detail below, the partition functions are determined by network topology and depend on additional parameters, including interaction strengths w, binding constants K, and "leakiness" q (i.e. the statistical weight given to bare binding of the RNAp). All parameters are positive. We first offer qualitative interpretation of the parameters, then we present the detailed expressions for the partition functions.

The w describe the interaction strengths between transcription factors, or between a transcription factor and the RNAp. Alphabetical superscripts refer to the promoter regions of genes A, B, or G, while numerical subscripts refer to the molecules involved in the interaction: RNAp (0), transcription factor A (1), or transcription factor B (2). For example, w^B_{01} describes the interaction between RNAp and transcription factor A at the promoter region of gene B.

The signs of the logs of the w^j_{0i} determine the signs of the edges (where $j \in \{A, B, G\}$ for the three promoter regions and $i \in \{1, 2\}$ for transcription factors A and B). For example, w^B_{01} describes the regulation of species B by species A; if $\log w^B_{01} > 0$ then the edge $A \to B$ is up-regulating, and if $\log w^B_{01} < 0$ then the edge $A \to B$ is down-regulating.

Following the model of Buchler et al. [1], when two transcription factors regulate one species, they may do so "independently" or "synergistically." Independent regulation corresponds to the case when both transcription factors interact with the same domain of the RNAp; mathematically the interaction strengths are additive ($w^j_{01} + w^j_{02}$). If the RNAp has several interaction domains, two transcription factors can interact synergistically, and the interaction strengths are multiplicative ($w^j_{01} w^j_{02}$). Synergistic regulation implies the additional constraint that the regulatory effects of the two transcription factors (i.e. the logs of the interaction strengths) are of the same sign.

The K describe the binding constants of each transcription factor to each promoter region. They have super- and subscripts similar to the w, e.g. K^B_1 describes the binding of transcription factor A to the promoter region of gene B.

In the next sections we give the forms of the partition functions $Z^j_{\text{on/off}}$ for the network

topologies shown in Fig. S1. To provide intuition, the first two expressions are interpreted in detail.

Topology A

Topology A is shown in Fig. S1A; its partition functions are

$$Z^A_{\text{on}} = q + w^A_{01} q \frac{a}{K^A_1}, \tag{11}$$

$$Z^A_{\text{off}} = 1 + \frac{a}{K^A_1}, \tag{12}$$

$$Z^B_{\text{on}} = q + w^B_{01} q \frac{a}{K^B_1}, \tag{13}$$

$$Z^B_{\text{off}} = 1 + \frac{a}{K^B_1}, \tag{14}$$

$$Z^G_{\text{on}} = q + w^G_{02} q \frac{b}{K^G_2}, \tag{15}$$

$$Z^G_{\text{off}} = 1 + \frac{b}{K^G_2}. \tag{16}$$

Eqn. 11 describes the two ways in which transcription can occur at the promoter region of gene A: (i) the RNAp can bind unassisted, with statistical weight q, or (ii) since A is self-regulating, the RNAp can bind upon interaction with transcription factor A, with weight proportional to q for the RNAp, to the effective concentration a scaled by the binding constant K^A_1 for transcription factor A, and to the interaction strength w^A_{01} between the RNAp and transcription factor A. Eqn. 12 describes the two ways in which transcription can not occur at the promoter region of gene A: (i) there can be nothing bound, an outcome whose statistical weight we are free, via the normalization enforced in Eqn. 10, to set, and so we set to 1, and (ii) the transcription factor alone can bind, with weight a/K^A_1. Eqns. 13-16 are similarly derived according to the topology of the network.

Topology B

Topology B is shown in Fig. S1B; its partition functions are

$$Z^A_{\rm on} = q + w^A_{02} q \frac{b}{K^A_2}, \tag{17}$$

$$Z^A_{\rm off} = 1 + \frac{b}{K^A_2}, \tag{18}$$

$$Z^B_{\rm on} = q + w^B_{01} q \frac{a}{K^B_1}, \tag{19}$$

$$Z^B_{\rm off} = 1 + \frac{a}{K^B_1}, \tag{20}$$

$$Z^G_{\rm on} = q + w^G_{02} q \frac{b}{K^G_2}, \tag{21}$$

$$Z^G_{\rm off} = 1 + \frac{b}{K^G_2}. \tag{22}$$

Topology C

Topology C is shown in Fig. S1C; its partition functions are

$$Z^A_{\rm on} = q + w^A_{01} q \frac{a}{K^A_1}, \tag{23}$$

$$Z^A_{\rm off} = 1 + \frac{a}{K^A_1}, \tag{24}$$

$$Z^B_{\rm on} = q + w^B_{01} q \frac{a}{K^B_1} + w^B_{02} q \frac{b}{K^B_2} + (w^B_{01} + w^B_{02}) w^B_{12} q \frac{a}{K^B_1} \frac{b}{K^B_2} \qquad \text{(additive)}, \tag{25}$$

$$Z^B_{\rm on} = q + w^B_{01} q \frac{a}{K^B_1} + w^B_{02} q \frac{b}{K^B_2} + w^B_{01} w^B_{02} w^B_{12} q \frac{a}{K^B_1} \frac{b}{K^B_2} \qquad \text{(multiplicative)}, \tag{26}$$

$$Z^B_{\rm off} = 1 + \frac{a}{K^B_1} + \frac{b}{K^B_2} + w^B_{12} \frac{a}{K^B_1} \frac{b}{K^B_2}, \tag{27}$$

$$Z^G_{\rm on} = q + w^G_{02} q \frac{b}{K^G_2}, \tag{28}$$

$$Z^G_{\rm off} = 1 + \frac{b}{K^G_2}. \tag{29}$$

Topology D

Topology D is shown in Fig. S1D; its partition functions are

$$Z^A_{\rm on} = q + w^A_{01} q \frac{a}{K^A_1} + w^A_{02} q \frac{b}{K^A_2} + (w^A_{01} + w^A_{02}) w^A_{12} q \frac{a}{K^A_1} \frac{b}{K^A_2} \qquad \text{(additive)}, \tag{30}$$

$$Z^A_{\rm on} = q + w^A_{01} q \frac{a}{K^A_1} + w^A_{02} q \frac{b}{K^A_2} + w^A_{01} w^A_{02} w^A_{12} q \frac{a}{K^A_1} \frac{b}{K^A_2} \qquad \text{(multiplicative)}, \tag{31}$$

$$Z^A_{\rm off} = 1 + \frac{a}{K^A_1} + \frac{b}{K^A_2} + w^A_{12} \frac{a}{K^A_1} \frac{b}{K^A_2}, \tag{32}$$

$$Z^B_{\rm on} = q + w^B_{01} q \frac{a}{K^B_1}, \tag{33}$$

$$Z^B_{\rm off} = 1 + \frac{a}{K^B_1}, \tag{34}$$

$$Z^G_{\rm on} = q + w^G_{02} q \frac{b}{K^G_2}, \tag{35}$$

$$Z^G_{\rm off} = 1 + \frac{b}{K^G_2}. \tag{36}$$

Topology E

Topology E is shown in Fig. S1E; its partition functions are

$$Z^A_{\rm on} = q + w^A_{02} q \frac{b}{K^A_2}, \tag{37}$$

$$Z^A_{\rm off} = 1 + \frac{b}{K^A_2}, \tag{38}$$

$$Z^B_{\rm on} = q + w^B_{01} q \frac{a}{K^B_1} + w^B_{02} q \frac{b}{K^B_2} + (w^B_{01} + w^B_{02}) w^B_{12} q \frac{a}{K^B_1} \frac{b}{K^B_2} \qquad \text{(additive)}, \tag{39}$$

$$Z^B_{\rm on} = q + w^B_{01} q \frac{a}{K^B_1} + w^B_{02} q \frac{b}{K^B_2} + w^B_{01} w^B_{02} w^B_{12} q \frac{a}{K^B_1} \frac{b}{K^B_2} \qquad \text{(multiplicative)}, \tag{40}$$

$$Z^B_{\rm off} = 1 + \frac{a}{K^B_1} + \frac{b}{K^B_2} + w^B_{12} \frac{a}{K^B_1} \frac{b}{K^B_2}, \tag{41}$$

$$Z^G_{\rm on} = q + w^G_{02} q \frac{b}{K^G_2}, \tag{42}$$

$$Z^G_{\rm off} = 1 + \frac{b}{K^G_2}. \tag{43}$$

Topology F

Topology F is shown in Fig. S1F; its partition functions are

$$Z^A_{\text{on}} = q + w^A_{01} q \frac{a}{K^A_1} + w^A_{02} q \frac{b}{K^A_2} + (w^A_{01} + w^A_{02}) w^A_{12} q \frac{a}{K^A_1} \frac{b}{K^A_2} \qquad \text{(additive)}, \tag{44}$$

$$Z^A_{\text{on}} = q + w^A_{01} q \frac{a}{K^A_1} + w^A_{02} q \frac{b}{K^A_2} + w^A_{01} w^A_{02} w^A_{12} q \frac{a}{K^A_1} \frac{b}{K^A_2} \qquad \text{(multiplicative)}, \tag{45}$$

$$Z^A_{\text{off}} = 1 + \frac{a}{K^A_1} + \frac{b}{K^A_2} + w^A_{12} \frac{a}{K^A_1} \frac{b}{K^A_2}, \tag{46}$$

$$Z^B_{\text{on}} = q + w^B_{01} q \frac{a}{K^B_1} + w^B_{02} q \frac{b}{K^B_2} + (w^B_{01} + w^B_{02}) w^B_{12} q \frac{a}{K^B_1} \frac{b}{K^B_2} \qquad \text{(additive)}, \tag{47}$$

$$Z^B_{\text{on}} = q + w^B_{01} q \frac{a}{K^B_1} + w^B_{02} q \frac{b}{K^B_2} + w^B_{01} w^B_{02} w^B_{12} q \frac{a}{K^B_1} \frac{b}{K^B_2} \qquad \text{(multiplicative)}, \tag{48}$$

$$Z^B_{\text{off}} = 1 + \frac{a}{K^B_1} + \frac{b}{K^B_2} + w^B_{12} \frac{a}{K^B_1} \frac{b}{K^B_2}, \tag{49}$$

$$Z^G_{\text{on}} = q + w^G_{02} q \frac{b}{K^G_2}, \tag{50}$$

$$Z^G_{\text{off}} = 1 + \frac{b}{K^G_2}. \tag{51}$$

Stochastic description: Linear noise approximation

The linear noise approximation (LNA) is a second-order expansion of the master equation made under the approximations that (i) mean protein numbers are large and (ii) fluctuations are small compared to means. Under the LNA, the steady state solution to the master equation is a Gaussian distribution: the first-order terms recover the deterministic system and thus provide the means, and the second-order terms yield an equation for the covariance matrix. Comprehensive discussions of the linear noise approximation can be found in [6–8].

Under the LNA the steady state distribution over each species' protein number is a Gaussian expansion around the deterministic mean given by the steady state of Eqns. 1-3. The covariance matrix Ξ is determined from model parameters by solving the Lyapunov equation

$$J\Xi + \Xi J^T + D = 0, \tag{52}$$

where J is the Jacobian of the system (Eqn. 4) and

$$D = \begin{pmatrix} R_A(\alpha + A) & 0 & 0 \\ 0 & R_B(\beta + B) & 0 \\ 0 & 0 & R_G(\gamma + G) \end{pmatrix} \tag{53}$$

is an effective diffusion matrix. We solve Eqn. 52 numerically using MATLAB's `lyap` function.

The deterministic steady state and the covariance matrix are computed four times (once in each of the chemical input states c); the lower-right terms of each provide the mean and variance, respectively, of each (Gaussian) output distribution $p(G|c)$. The input-output mutual information is computed directly from the distributions $p(G|c)$, as described next.

INFORMATION THEORY

In this study we make use of a central measure from information theory: *mutual information* (MI). MI is a fundamental measure of the strength a relationship between two random variables. More precisely, it measures the reduction in entropy of one variable given measurement of the other. MI captures correlation between two random variables even when a relationship exists that is nonlinear (unlike, e.g., the correlation coefficient) or non-monotonic (unlike, e.g., Spearman's rho). It has found wide use in the study of biological networks both as a statistical measure [9, 10] and as a measure of functionality in the presence of noise [11–13]. For a comprehensive review of information theory we refer the reader to [14].

In this study we employ MI in two separate contexts: (i) as a measure of network functionality and (ii) as a measure of statistical correlation. In the first context, we optimize the MI between the chemical input state and the concentration of the output protein. In the second context, we compute, for a given topological feature (e.g. number of up-regulations), the MI between the value that the feature takes in a network and the function that the network performs. We here describe these computations in turn.

MI is the average of the log of a ratio. The average is over the joint probability distribution between two random variables, and the ratio is that of the joint to the product of the marginal distributions. For a discrete variable, i.e. the chemical input state c, and a continuous

variable, i.e. the output protein concentration G, MI takes the form

$$I[p(c,G)] = \sum_c \int dG\, p(c,G) \log_2 \frac{p(c,G)}{p(c)p(G)}, \tag{54}$$

where the log is taken in base 2 to give I in bits. Noting that $p(c,G) = p(G|c)p(c)$ and $p(G) = \sum_c p(c,G)$ allows one to write the MI as

$$I[p(c,G)] = \sum_c \int dG\, p(G|c)p(c) \log_2 \frac{p(G|c)}{\sum_{c'} p(G|c')p(c')}, \tag{55}$$

i.e. entirely in terms of the conditional output distributions $p(G|c)$, obtained via the linear noise approximation (see above), and the input distribution $p(c)$, which we take as $p(c) = 1/4$ for equally likely chemical input states. Eqn. 55 is integrated numerically during the optimization using MATLAB's `quad`.

In the context of correlating, for a topological feature μ, the feature value v_μ with the observed function r, since both are categorical (and therefore discrete) variables, MI takes the form

$$I[p(v_\mu,r)] = \sum_{v_\mu,r} p(v_\mu,r) \log \frac{p(v_\mu,r)}{p(v_\mu)p(r)}. \tag{56}$$

Here, the joint distribution $p(v_\mu,r)$ is computed from the optimization data according to Eqn. 2 of the main text, and the marginal distributions are trivially obtained as $p(v_\mu) = \sum_r p(v_\mu,r)$ and $p(r) = \sum_{v_\mu} p(v_\mu,r)$.

Additionally we note that MI is again used in the context of statistical correlation to compute a feature adjacency matrix (see *Non-redundant features* below). That is, the MI between the values of a feature μ and a feature ν is given by

$$I[p(v_\mu,v_\nu)] = \sum_{v_\mu,v_\nu} p(v_\mu,v_\nu) \log \frac{p(v_\mu,v_\nu)}{p(v_\mu)p(v_\nu)}, \tag{57}$$

where $p(v_\mu,v_\nu)$ is computed directly from the network set.

OPTIMIZATION

Optimization of input-output information $I[p(G,c)]$ (Eqn. 55) over model parameters is done numerically using MATLAB's `fminsearch`. Each optimization is performed at constrained average protein number $N \equiv (A+B+G)/3$ and average timescale separation $T \equiv [(R_A+R_B)/2]/R_G$ by maximizing the quantity

$$L \equiv I[p(G,c)] - \eta N - \kappa T \tag{58}$$

Parameter	Bounds
Promoter strengths, s	$10^{-4} - 10^{6}$
Interaction strengths, $w > 1$ (up-regulation)	$1.05 - 10^{2}$
Interaction strengths, $w < 1$ (down-regulation)	$10^{-2} - 0.95$
Binding constants, K	$10^{-1} - 10^{2}$
Leakiness, q	$10^{-10} - 10^{-2}$
Scaling factors, $x > 1$, $y > 1$	$1.1 - 10^{4}$
Degradation rates, R_A, R_B	$10^{-7} - 10^{0}$
Degradation rate, R_G (fixed)	$4 \cdot 10^{-4}$

TABLE S1: Bounds from which parameters are drawn to initialize optimization.

for values of the Lagrange multipliers η and κ which give biologically plausible values for N and T for single cells (R_G is fixed). The optimization is initialized by sampling uniform-randomly in the logs of the parameters; bounds from which initial parameters are drawn are given in Table S1.

ROBUSTNESS OF ρ RANKING

The correlation between topological feature value v_μ and network function r is measured for each feature μ using a normalized mutual information ρ_μ. This measure is a function of the joint distribution $p(v_\mu, r)$, whose computation (Eqn. 2 of main text) depends on two distributions which we take to be uniform: (i) $p(n)$, the probability of observing each network n, and (ii) $p(\vartheta|n)$, the probability of observing each optimally functional point ϑ in the parameter space of network n. Here we show that the ranking of the ρ_μ is robust to perturbations in the uniformity of each of these distributions.

Perturbing $p(n)$

The uniformity of $p(n)$ is perturbed by artificially setting $p(n) \propto (u_n)^\epsilon$, where u_n is a vector of random numbers and ϵ tunes the entropy of the distribution $H[p(n)]$. That is, $\epsilon = 0$ recovers the maximum-entropy (uniform) distribution, while $\epsilon \to \infty$ produces the zero-entropy solution $p(n) \to \delta(n, \text{argmax}\, u_n)$ (where δ is the Kronecker delta). Fig. S2A

plots the ρ_μ as a function of the entropy $H[p(n)]$. As seen in Fig. S2A, the ranking of the top 4 features is preserved under $\sim$15% perturbations in the entropy, and that of the top 3 features is preserved under $\sim$30% perturbations. This demonstrates that the feature ranking is considerably robust to perturbations in the uniformity of $p(n)$.

Perturbing $p(\vartheta|n)$

The uniformity of $p(\vartheta|n)$ for each network n is perturbed via the same procedure described in the previous section. Fig. S2B plots the ρ_μ as a function of the entropy of $p(\vartheta) = \sum_n p(\vartheta|n)p(n)$, where $p(n)$ here is uniform. As seen in Fig. S2B, the ranking of the top 7 features is preserved under $\sim$40% perturbations in the entropy of $p(\vartheta)$, indicating that the feature ranking is very robust to perturbations in $p(\vartheta|n)$.

In this case we also have an independent entropy scale, given by the fact that we may decompose $p(\vartheta|n)$ as

$$p(\vartheta|n) = \sum_{\vartheta_0} p(\vartheta|\vartheta_0, n)p(\vartheta_0|n), \tag{59}$$

where ϑ_0 is the parameter setting that initializes an optimization and $p(\vartheta|\vartheta_0, n)$ is determined by the optimization itself. If we assume uniformity of $p(\vartheta_0|n)$, instead of $p(\vartheta|n)$, then $p(\vartheta|n)$ is computable from the numbers of times the optimization converges repeatedly on each local optimum ϑ. The entropy in this case is 13% different from that of the uniform distribution, and the ranking of ρ is almost entirely unchanged (Fig. S2B). Fig. S2B demonstrates that the results are not sensitive to whether one takes the distribution of initial parameters or the distribution of optimal parameters to be uniform.

NON-REDUNDANT FEATURES

To interpret which features are associated with which sets of realizable functions, it is useful to group nearly identical features together and use only the feature which is most informative about function (highest in ρ) as the exemplar among each group. To quantify redundancy among features, we compute the MI between each pair of features and normalize by the minimum entropy to produce a weighted adjacency matrix

$$M_{\mu\nu} = \frac{I[p(v_\mu, v_\nu)]}{\min\{H[p(v_\mu)], H[p(v_\nu)]\}} \tag{60}$$

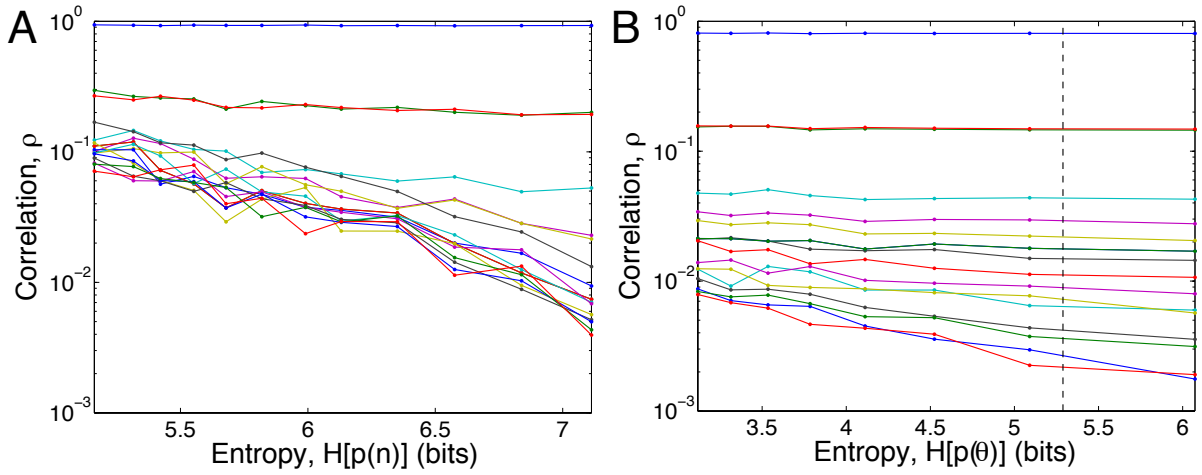

FIG. S2: Values of the correlation measure ρ for each of the 17 features as a function of the entropies (A) $H[p(n)]$ and (B) $H[p(\vartheta|n)]$. Each point represents the average of 8 trials. In B, the dashed vertical line shows the entropy under the assumption that $p(\vartheta_0|n)$, not $p(\vartheta|n)$, is uniform.

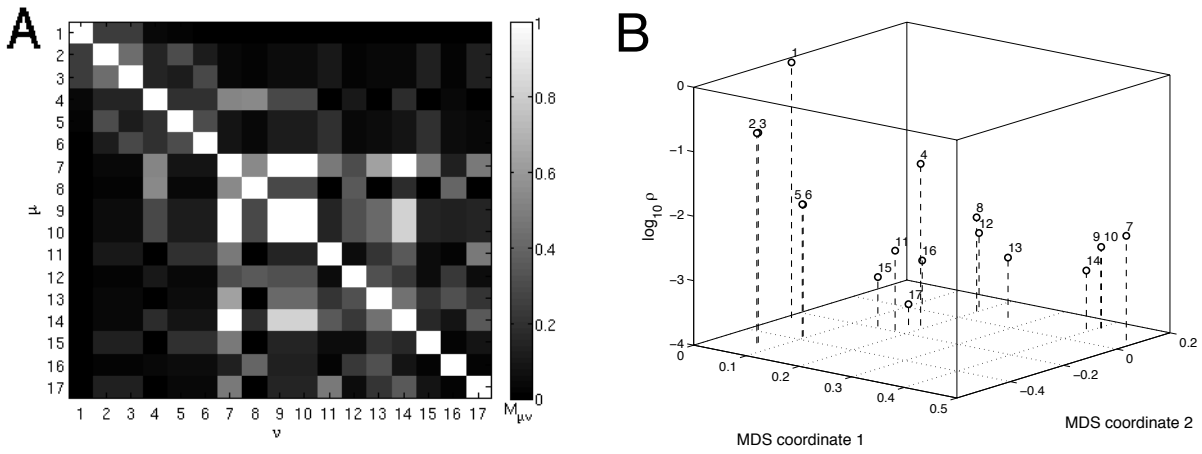

FIG. S3: Identifying non-redundant topological features. (A) Feature adjacency matrix (Eqn. 60). (B) Features plotted according to correlation measure ρ and the coordinates of a two-dimensional scaling based on the adjacency matrix in A. Features are numbered as in Table 1 of the main text.

(Fig. S3A). We then use the adjacency matrix as the basis for multidimensional scaling, as described below.

Multidimensional scaling (MDS) describes a class of techniques used to visualize proximities among data in a low-dimensional space. One of the most common techniques (also called principal components analysis when applied to a correlation matrix) is to use as the low-dimensional coordinates the eigenvectors of the adjacency matrix corresponding to the largest-magnitude eigenvalues. Data points with high mutual proximity then tend to be

grouped together along these coordinates. Fig. S3B here and Fig. 5 of the main text show the application of this technique in two and one dimensions, respectively, to the adjacency matrix in Fig. S3A, revealing groups of similar features. Plotting the feature-function correlation measure ρ along the vertical axis in each case makes apparent the most informative feature in each group (i.e. feature 1 in one group and feature 4 in a second group).

DIRECT FUNCTIONALITY: VALIDATION OF KNOWN ANALYTIC RESULT

In previous work [15] we show analytically that networks in which each species is regulated by at most one other species perform only "direct" functions, in which the sign of the effect of an input species on an output species depends only on the direct path from input to output, even when there is feedback. This analytic result is here validated by our statistical approach.

In the context of our setup (see Fig. 1A of the main text), the direct paths from the inputs (the chemical inhibitors labeled by x and y) to the output (the fluorescent protein G) involve only the forward regulatory edges $A \to B$ and $B \to G$. Therefore considering only those networks in which each species is singly regulated (Fig. S1A-B), the analytic result predicts that the signs of the forward edges uniquely determine the type of function performed. Plotting the conditional distribution $p(r|v)$ for the feature 'signs of the forward edges' using only data from these networks confirms that this is indeed the case (Fig. S4). Accordingly the correlation for this distribution is $\rho = 1$, the maximum possible value.

The functions performed at each of the feature values in Fig. S4 can be understood intuitively. For example, in networks with the last feature value $A \multimap B \multimap G$, inhibition of A and of B will both reduce the expression of G, such that the state in which both small molecules are present $(++)$ produces the lowest-ranked output, and conversely, the state in which both small molecules are absent $(--)$ produces the highest-ranked output; one may verify by inspection that functions 7 and 8 are the two that satisfy these criteria. The correspondence of the other function pairs to feature values can be similarly understood in terms of the edge signs.

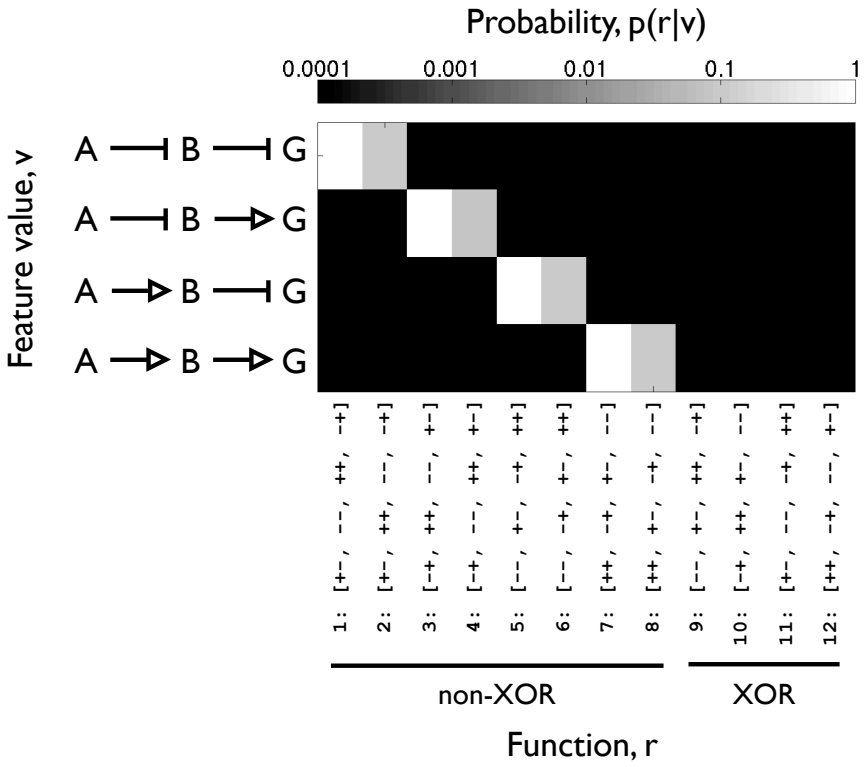

FIG. S4: Conditional distribution showing the probability of a particular input-output function given the value of the topological feature 'signs (up- or down-regulating) of the forward regulatory edges,' using only data from networks in which each species is singly regulated (Fig. S1A-B). Only direct functions are performed, as defined in the text.

XOR FUNCTIONALITY: ANALYSIS

As described in the main text, XOR functions satisfy one or both of two properties:

$$\text{XOR property I}: \ \text{sign}\,(dG/dx) \ \text{depends on } y, \tag{61}$$

$$\text{XOR property II}: \ \text{sign}\,(dG/dy) \ \text{depends on } x. \tag{62}$$

To analytically understand the observed XOR functionality, we here calculate the derivatives dG/dx and dG/dy from the steady state of the deterministic system (Eqns. 1-3). We further show how the forms of these derivatives support the observations that (i) all XOR functions satisfying property I are performed by networks in which species B is autoregulated, and (ii) no functions satisfying property II are observed.

Calculating the derivatives

The steady state of Eqns. 1-3, with all functional dependencies made explicit, is

$$A = \alpha[a(A,x), b(B,y)], \tag{63}$$

$$B = \beta[a(A,x), b(B,y)], \tag{64}$$

$$G = \gamma[b(B,y)], \tag{65}$$

where $a(A,x) = A/x$ and $b(B,y) = B/y$. The output G depends on the input x only through b, and b depends on x only through B, i.e.

$$\frac{dG}{dx} = \frac{d\gamma}{dx} = \frac{d\gamma}{db}\frac{\partial b}{\partial B}\frac{dB}{dx}. \tag{66}$$

The dependencies of A and B on x are coupled:

$$\frac{dA}{dx} = \frac{d\alpha}{dx} = \frac{\partial\alpha}{\partial a}\frac{da}{dx} + \frac{\partial\alpha}{\partial b}\frac{db}{dx} \tag{67}$$

$$= \frac{\partial\alpha}{\partial a}\left(\frac{\partial a}{\partial A}\frac{dA}{dx} + \frac{\partial a}{\partial x}\right) + \frac{\partial\alpha}{\partial b}\left(\frac{\partial b}{\partial B}\frac{dB}{dx}\right), \tag{68}$$

$$\frac{dB}{dx} = \frac{d\beta}{dx} = \frac{\partial\beta}{\partial a}\frac{da}{dx} + \frac{\partial\beta}{\partial b}\frac{db}{dx} \tag{69}$$

$$= \frac{\partial\beta}{\partial a}\left(\frac{\partial a}{\partial A}\frac{dA}{dx} + \frac{\partial a}{\partial x}\right) + \frac{\partial\beta}{\partial b}\left(\frac{\partial b}{\partial B}\frac{dB}{dx}\right). \tag{70}$$

Eqns. 68 and 70 form an algebraic system of equations in the variables dA/dx and dB/dx, whose solution is

$$\frac{dA}{dx} = \frac{1}{-\Delta}\left[\frac{\partial\alpha}{\partial a}\frac{\partial a}{\partial x}\left(1 - \frac{\partial\beta}{\partial b}\frac{\partial b}{\partial B}\right) + \frac{\partial\alpha}{\partial b}\frac{\partial b}{\partial B}\frac{\partial\beta}{\partial a}\frac{\partial a}{\partial x}\right], \tag{71}$$

$$\frac{dB}{dx} = \frac{1}{-\Delta}\frac{\partial\beta}{\partial a}\frac{\partial a}{\partial x}, \tag{72}$$

where

$$\Delta = \left(\frac{\partial\alpha}{\partial b}\frac{\partial b}{\partial B}\right)\left(\frac{\partial\beta}{\partial a}\frac{\partial a}{\partial A}\right) - \left(\frac{\partial\alpha}{\partial a}\frac{\partial a}{\partial A} - 1\right)\left(\frac{\partial\beta}{\partial b}\frac{\partial b}{\partial B} - 1\right) \tag{73}$$

$$= \frac{\partial\alpha}{\partial B}\frac{\partial\beta}{\partial A} - \left(\frac{\partial\alpha}{\partial A} - 1\right)\left(\frac{\partial\beta}{\partial B} - 1\right) \tag{74}$$

is the determinant of the Jacobian of the dynamical system and is always negative at stable fixed points (Eqn. 6). Substituting Eqn. 72 into Eqn. 66 and using $\partial\gamma/\partial B = (\partial\gamma/\partial b)(\partial b/\partial B)$ yields Eqn. 4 of the main text,

$$\frac{dG}{dx} = \frac{1}{-\Delta}\frac{\partial a}{\partial x}\frac{\partial\beta}{\partial a}\frac{\partial\gamma}{\partial B}. \tag{75}$$

The output G depends on the input y through b, which depends on y either indirectly through B or directly, i.e.

$$\frac{dG}{dy} = \frac{d\gamma}{dy} = \frac{d\gamma}{db}\frac{db}{dy} = \frac{d\gamma}{db}\left(\frac{\partial b}{\partial B}\frac{dB}{dy} + \frac{\partial b}{\partial y}\right). \tag{76}$$

As on x, the dependencies of A and B on y are coupled:

$$\begin{aligned}
\frac{dA}{dy} &= \frac{d\alpha}{dy} = \frac{\partial\alpha}{\partial a}\frac{da}{dy} + \frac{\partial\alpha}{\partial b}\frac{db}{dy} && (77)\\
&= \frac{\partial\alpha}{\partial a}\left(\frac{\partial a}{\partial A}\frac{dA}{dy}\right) + \frac{\partial\alpha}{\partial b}\left(\frac{\partial b}{\partial B}\frac{dB}{dy} + \frac{\partial b}{\partial y}\right), && (78)\\
\frac{dB}{dy} &= \frac{d\beta}{dy} = \frac{\partial\beta}{\partial a}\frac{da}{dy} + \frac{\partial\beta}{\partial b}\frac{db}{dy} && (79)\\
&= \frac{\partial\beta}{\partial a}\left(\frac{\partial a}{\partial A}\frac{dA}{dy}\right) + \frac{\partial\beta}{\partial b}\left(\frac{\partial b}{\partial B}\frac{dB}{dy} + \frac{\partial b}{\partial y}\right). && (80)
\end{aligned}$$

Eqns. 78 and 80 can be solved to yield

$$\begin{aligned}
\frac{dA}{dy} &= \frac{1}{-\Delta}\frac{\partial\alpha}{\partial b}\frac{\partial b}{\partial y}, && (81)\\
\frac{dB}{dy} &= \frac{1}{-\Delta}\left[\frac{\partial\beta}{\partial b}\frac{\partial b}{\partial y}\left(1 - \frac{\partial\alpha}{\partial a}\frac{\partial a}{\partial A}\right) + \frac{\partial\beta}{\partial a}\frac{\partial a}{\partial A}\frac{\partial\alpha}{\partial b}\frac{\partial b}{\partial y}\right], && (82)
\end{aligned}$$

where Δ is the determinant as in Eqn. 74. Substituting Eqn. 82 into Eqn. 76 and simplifying gives Eqn. 5 of the main text,

$$\frac{dG}{dy} = \frac{1}{-\Delta}\left(1 - \frac{\partial\alpha}{\partial A}\right)\frac{\partial b}{\partial y}\frac{d\gamma}{db}, \tag{83}$$

where $\partial\alpha/\partial A = (\partial\alpha/\partial a)(\partial a/\partial A)$.

Type-I XOR functions require autoregulation of B

Type-I XOR functionality (Eqn. 61) requires the sign of the derivative dG/dx (Eqn. 75) to depend on y. Here we go through each term in Eqn. 75 and conclude that only the third can change sign. The first term in Eqn. 75, $1/(-\Delta)$, is always positive because the determinant Δ is equal to the product of the three eigenvalues of the Jacobian of the deterministic system, which at a stable fixed point are all negative (Eqn. 6). The second term in Eqn. 75 is $\partial a/\partial x = -A/x^2$, which is always negative, corresponding to the inhibitory effect of the small molecule x on transcription factor A. The fourth term in Eqn. 75 is $\partial\gamma/\partial B = (\partial\gamma/\partial b)(\partial b/\partial B)$. The factor $\partial b/\partial B = 1/y$ is always positive, and the factor

$\partial\gamma/\partial b$ is of unique sign because $\gamma(b)$ is monotonic, as shown below. This leaves only the third term, $\partial\beta/\partial a$, which can change sign if and only if B is autoregulated, as discussed below.

Under our model a regulation function with only one argument is monotonic, which is consistent with the interpretation of the edge being either up- or down-regulating. For example, the regulation function corresponding to the edge $B \to G$ in all networks is (see Eqns. 9-10)

$$\gamma(b) = \frac{s_G}{R_G} \frac{Z^G_{\text{on}}}{Z^G_{\text{on}} + Z^G_{\text{off}}}, \tag{84}$$

where Z^G_{on} and Z^G_{off} are given by, e.g., Eqns. 15-16. The derivative of this function with respect to its argument is

$$\frac{d\gamma}{db} = \frac{s_G}{R_G Z_G^2} \left(\frac{dZ^G_{\text{on}}}{db} Z^G_{\text{off}} - Z^G_{\text{on}} \frac{dZ^G_{\text{off}}}{db} \right), \tag{85}$$

where $Z_G = Z^G_{\text{on}} + Z^G_{\text{off}}$. Upon differentiating and inserting Eqns. 15 and 16, all dependence on b inside the parentheses cancels, leaving

$$\frac{d\gamma}{db} = \frac{s_G q}{R_G K_2^G Z_G^2} (w^G_{02} - 1). \tag{86}$$

Eqn. 86 confirms that $\gamma(b)$ is monotonic, with $w^G_{02} > 1$ corresponding to up-regulation, and $w^G_{02} < 1$ corresponding to down-regulation.

If species B is not autoregulated, then it is only regulated by species A; the regulation function then only has one argument, i.e. $\beta(a, b) = \beta(a)$, and, as with $\gamma(b)$ above, it is monotonic. Therefore without autoregulation of B, type-I XOR functionality is not possible. We now compute the derivative $\partial\beta/\partial a$ in the case of two arguments to analytically demonstrate the converse: that with autoregulation of B, type-I XOR functionality is possible.

As with Eqn. 85, the partial derivative of $\beta(a, b)$ with respect to a takes the form

$$\frac{\partial\beta}{\partial a} = \frac{s_B}{R_B Z_B^2} \left(\frac{\partial Z^B_{\text{on}}}{\partial a} Z^B_{\text{off}} - Z^B_{\text{on}} \frac{\partial Z^B_{\text{off}}}{\partial a} \right), \tag{87}$$

where $Z_B = Z^B_{\text{on}} + Z^B_{\text{off}}$, Z^B_{on} (with B autoregulated) is given by, e.g., Eqn. 25 for additive interaction and Eqn. 26 for multiplicative interaction, and Z^B_{off} is given by, e.g., Eqn. 27. Upon differentiating and inserting the expressions for Z^B_{on} and Z^B_{off}, all dependence on a inside the parentheses cancels (for both additive and multiplicative interaction), leaving

$$\frac{\partial\beta}{\partial a} = \frac{s_B q}{R_B K_1^B Z_B^2} \left(C_2 b^2 + C_1 b + C_0 \right), \tag{88}$$

where for additive interaction,

$$C_0 = w_{01}^B - 1, \tag{89}$$

$$C_1 = \frac{1}{K_2^B}\left[w_{01}^B - w_{02}^B - w_{12}^B + \left(w_{01}^B + w_{02}^B\right) w_{12}^B\right], \tag{90}$$

$$C_2 = \left(\frac{1}{K_2^B}\right)^2 w_{01}^B w_{12}^B, \tag{91}$$

and for multiplicative interaction,

$$C_0 = w_{01}^B - 1, \tag{92}$$

$$C_1 = \frac{1}{K_2^B}\left[w_{01}^B - w_{02}^B - w_{12}^B + w_{01}^B w_{02}^B w_{12}^B\right], \tag{93}$$

$$C_2 = \left(\frac{1}{K_2^B}\right)^2 \left(w_{01}^B - 1\right) w_{02}^B w_{12}^B. \tag{94}$$

Eqn. 88 is the product of a positive term and a quadratic function of $b = B/y$. It is straightforward to demonstrate in both the additive and multiplicative cases (e.g. by sampling numerically) that for positive w_{01}^B, w_{02}^B, and w_{12}^B the quadratic function can have positive, negative, or complex roots. When at least one root is positive, the sign of $\partial\beta/\partial a$ changes at positive B/y, i.e. the sign can depend on y. Since dG/dx is proportional to $\partial\beta/\partial a$ (Eqn. 75), this enables type-I XOR functionality. This analysis suggests inspection of the parameters themselves obtained via optimization; doing so, we observe that the vast majority of observed XOR functions results from optimal parameter values for which there exists a positive root in the range $0 < B/y < \sim 100$, which is precisely the range of protein numbers in which our optimal solutions lie.

To summarize, nonmonotonicity in the regulation of species B, which can occur only when B is autoregulated, produces the observed XOR functions.

Type-II XOR functions are not observed

Type-II XOR functionality (Eqn. 62) requires the sign of the derivative dG/dy (Eqn. 83) to depend on x. Three of the terms in Eqn. 83 are of unique sign: the terms $1/(-\Delta)$ and $d\gamma/db$ are positive and of unique sign respectively, as discussed in the previous section; and the term $\partial b/\partial y = -B/y^2$ is always negative, corresponding to the inhibitory effect of the small molecule y on transcription factor B. This leaves only the term $(1 - \partial\alpha/\partial A)$, which, as discussed below, for four of the network topologies is provably positive at stable fixed

points, and for the other two network topologies is observed to be positive for all optimal solutions.

For topologies B and E (Fig. S1), in which $\partial\alpha/\partial A = 0$, the term $(1 - \partial\alpha/\partial A) = 1$ is clearly positive. For topologies A and C, in which $\partial\alpha/\partial B = 0$, the first eigenvalue of the Jacobian (Eqn. 5) reduces to $\lambda_1 = \partial\alpha/\partial A - 1$; since this must be negative for stability, the term $(1 - \partial\alpha/\partial A)$ is always positive for these topologies as well. This leaves only networks with topology D or F.

In networks with topology D or F, It is unclear whether type-II XOR functions are analytically forbidden or simply exceedingly improbable for optimally informative parameters. Some analytic constraints can be obtained by the facts that since the real parts of λ_1 and λ_2 (Eqn. 5) are negative at stable fixed points, their sum must be negative and their product must be positive, i.e.

$$-(\lambda_1 + \lambda_2) = \left(1 - \frac{\partial\alpha}{\partial A}\right) + \left(1 - \frac{\partial\beta}{\partial B}\right) > 0. \tag{95}$$

$$\lambda_1\lambda_2 = \left(1 - \frac{\partial\alpha}{\partial A}\right)\left(1 - \frac{\partial\beta}{\partial B}\right) - \frac{\partial\alpha}{\partial B}\frac{\partial\beta}{\partial A} > 0. \tag{96}$$

If $(1 - \partial\beta/\partial B) < 0$, then Eqn. 95 implies that $(1 - \partial\alpha/\partial A) > 0$, forbidding type-II XOR functions. If on the other hand $(1 - \partial\beta/\partial B) > 0$, Eqn. 95 does not restrict the sign of $(1 - \partial\alpha/\partial A)$, but Eqn. 96 implies

$$\left(1 - \frac{\partial\alpha}{\partial A}\right) > \frac{(\partial\alpha/\partial B)(\partial\beta/\partial A)}{1 - \partial\beta/\partial B}. \tag{97}$$

Although in this last case it is not known whether the right-hand side is constrained to be positive, empirically the term $(1 - \partial\alpha/\partial A) > 0$ is observed to be positive for all optimal solutions, even over wide variations in the orders of magnitude of each of the optimal parameters across solutions.

[1] Buchler, NE, Gerland, U, Hwa, T (2003) On schemes of combinatorial transcription logic. *Proc Natl Acad Sci USA* 100:5136–41.

[2] Bintu, L et al. (2005) Transcriptional regulation by the numbers: models. *Curr Opin Genet Dev* 15:116–24.

[3] Bintu, L et al. (2005) Transcriptional regulation by the numbers: applications. *Curr Opin Genet Dev* 15:125–35.

[4] Guptasarma, P (1995) Does replication-induced transcription regulate synthesis of the myriad low copy number proteins of escherichia coli? *Bioessays* 17:987–97.

[5] Gillespie, DT (1977) Exact stochastic simulation of coupled chemical reactions. *J Phys Chem* 81:2340–2361.

[6] van Kampen, NG (1992) *Stochastic processes in physics and chemistry* (Amsterdam: North-Holland).

[7] Elf, J, Ehrenberg, M (2003) Fast evaluation of fluctuations in biochemical networks with the linear noise approximation. *Genome Research* 13:2475–84.

[8] Paulsson, J (2004) Summing up the noise in gene networks. *Nature* 427:415–8.

[9] Margolin, AA et al. (2006) ARACNE: an algorithm for the reconstruction of gene regulatory networks in a mammalian cellular context. *BMC Bioinformatics* 7:S7.

[10] Ziv, E, Middendorf, M, Wiggins, CH (2005) Information-theoretic approach to network modularity. *Physical Review E* 71:046117.

[11] Tkacik, G, Callan, CG, Bialek, W (2008) Information flow and optimization in transcriptional regulation. *Proc Natl Acad Sci USA* 105:12265–70.

[12] Mehta, P, Goyal, S, Long, T, Bassler, BL, Wingreen, NS (2009) Information processing and signal integration in bacterial quorum sensing. *Mol Syst Biol* 5:325.

[13] Walczak, AM, Tkačik, G, Bialek, W (2010) Optimizing information flow in small genetic networks. II. Feed-forward interactions. *Phys. Rev. E* 81:41905.

[14] Cover, TM, Thomas, JA (1991) *Elements of Information Theory* (John Wiley and Sons, New York, NY).

[15] Mugler, A, Ziv, E, Nemenman, I, Wiggins, C (2008) Serially regulated biological networks fully realise a constrained set of functions. *Systems Biology, IET* 2:313–322.